SCIPEDIA Revista Internacional de Métodos Numéricos para Cálculo y Diseño en Ingeniería

Revista Internacional Métodos numéricos para cálculo y diseño en ingeniería RIMNI CIMNE

A New Dynamical Analysis of COVID-19 Epidemic Model Using Two Fractional Operators

Ahmed Hagag[1], **Zuhur Alqahtani**[2,*] **and Anas Arafa**[3,4]

[1]Department of Basic Science, Faculty of Engineering, Sinai University, Kantara Branch, Ismailia, 41636, Egypt

[2]Department of Mathematical Sciences, College of Science, Princess Nourah bint Abdulrahman University, P.O. Box 84428, Riyadh, 11671, Saudi Arabia

[3]Department of Mathematics, College of Science, Qassim University, Buraydah, 51452, Saudi Arabia

[4]Department of Mathematics, Faculty of Science, Port Said University, Port Said, 42511, Egypt

ABSTRACT

Fractional calculus has emerged as a powerful tool for modeling complex systems with memory and hereditary properties, particularly in biological and epidemiological contexts. Despite its potential, accurately capturing the dynamics of diseases like COVID-19 remains challenging due to the need for models that balance accuracy with computational efficiency. This study presents a new dynamic analysis of the fractional-order coronavirus (2019-nCOV) pandemic model. The model incorporates two fractional derivatives, the Caputo and Atangana-Baleanu in Caputo sense (ABC) derivatives. By applying the Fractional Temimi-Ansari Method (FTAM), we derive a power series solution, demonstrating the existence, uniqueness, and convergence of the solutions. Our findings indicate that the fractional derivatives, particularly the ABC derivative, offer a more comprehensive description of memory effects in biological systems, which is crucial for accurately modeling the dynamics of COVID-19. The results show a high degree of accuracy and efficiency in capturing the behavior of the system, with convergence analyses confirming the robustness of the model. Graphical representations further illustrate the system's behavior under different parameter settings. The proposed model also effectively simulates the spread of the virus in Ghana, offering valuable insights for implementing non-pharmaceutical interventions. These findings demonstrate the potential of fractional calculus in improving epidemic models, especially in capturing the long-term effects and memory characteristics of pandemics.

OPEN ACCESS

Received: 31/08/2024

Accepted: 01/11/2024

DOI
10.23967/j.rimni.2024.10.57948

Keywords:
Caputo fractional derivative
atangana baleanu fractional derivative in Caputo sense
coronavirus (2019-nCOV)
fractional temimi-ansari method (FTAM)

1 Introduction

Mathematical modeling of infectious diseases has evolved greatly over the past three decades and is still growing in different fields such as epidemiology [1–4]. Diseases pose a great danger to people

*Correspondence: Zuhur Alqahtani (zumalqahtani@pnu.edu.sa).

as well as to a nation's economy. A proper understanding of disease dynamics plays a critical role in reducing infection in the general population.

Mathematical models have been recognized as serviceable paraphernalia that can assist decision-makers in global public health institutes more than ever [5]. The COVID-19 was initially reported in Wuhan, China. It has been seen that COVID-19 is transmitted from animals to humans, as many infected people were told that they were on 28 November at a local fish and wildlife market in Wuhan [6]. Sooner, some researchers have proven that transmission also occurs from one individual to the other [7].

However, basic solutions to these equations have desirable scaling qualities that make them appealing to implementations. Egypt topped the scene, as it was the first African country to record the first case of coronavirus infection on 14 February 2020 [8]. Then followed the injuries until Ghana recorded its first injury on 12 March 2020 [8].

Then the infected cases continued until Ghana documented 12,929 affirmed cases, involving 66 deaths, and 4468 recoveries with 8395 active people, as of 18 June 2020 [9]. Keep in mind that risk factors were also implicated in these fatalities, for example, diabetes, cardiovascular disease, and hypertension [9].

Asamoah et al. [10] studied the classic model of COVID-19 using data from Ghana, which has contributed significantly to current knowledge about the spread of COVID-19 and the dynamic impact of the virus on the ocean through humanitarian actions in Ghana. It will also help the government and the system see the ideal pathway to implement non-drug interventions.

The coronavirus transmission system (SEAIRV model) of non-partial arrangement is given in [10] by the following system of normal differential equations:

$$\begin{cases} \dfrac{dS}{dt} = \Lambda - \omega S - \beta\left[IS + \eta AS\right] - \beta_1 VS + \rho R, \\ \dfrac{dE}{dt} = \beta\left[IS + \eta AS\right] + \beta_1 VS - E\left\{k_2(1-\gamma) + k_1\gamma + \omega\right\}, \\ \dfrac{dA}{dt} = k_2(1-\gamma)E - A\left\{\omega + v_1\varphi + v_2(1-\varphi)\right\}, \\ \dfrac{dI}{dt} = k_1\gamma E + v_1\varphi A - I\left\{\epsilon + \omega + \alpha\right\}, \\ \dfrac{dR}{dt} = v_2(1-\varphi)A + \epsilon I - R(\rho + \omega), \\ \dfrac{dV}{dt} = m_1 A + m_2 I - \tau V, \end{cases} \tag{1}$$

with initial conditions

$$S_0(0) = 30416000,\ E_0(0) = 5,\ A_0(0) = 5,\ I_0(0) = 2,\ R_0(0) = 0,\ V_0(0) = 0, \tag{2}$$

where the susceptible population is denoted by S, E denotes the exposed population,

A indicates the asymptomatic population, I represents the population with symptoms, R denotes the recovered population and V indicates the virus on surfaces in the vicinity. The total number of individuals, $G(t)$ at time t is given as:

$$G(t) = S(t) + E(t) + A(t) + I(t) + R(t).$$

Table 1 illustrates the parameters in the model (1) and gives the rates for the evaluated parameters.

Table 1: Evaluated parameter rates for the coronavirus (SEAIRV) model (1)

Parameter		Range	Baseline worth	Reference
Λ	Recruitment rate	1319.294 day^{-1}	1319.294	[11,12]
ω	Natural death rate	4.2578E5 day^{-1}	4.2578E5	[9]
β	Transmission rate	6.038E–8: 0.8038	6.038E–8	Estimated
β_1	Transmission rate from the environment	4.00199E–8	4.00199E–8	Estimated
η	Proportional transmission to asymptomatic individuals	0.62811041: 0.6366 day^{-1}	0.6323	Estimated
ρ	How quickly the healed individuals access vulnerable groups	0.41138431 day^{-1}	0.41138431	Estimated
k_1	Progress rate from exposure with the symptomatic (highly infected) group	0.1923: 0.07142238 day^{-1}	0.1318	Estimated
k_2	Progress rate from exposure with the asymptomatic group	0.1763: 0.14285824 day^{-1}	0.1596	Estimated
γ	Percentage of people who receive prompt diagnosis	0.01: 0.0648	0.0374	Estimated
v_1	Progress rate from asymptomatic with the symptomatic class	0.1929: 0.2 day^{-1}	0.1965	Estimated
v_2	Advancement from asymptomatic to the recovered group	0.79999398 day^{-1}	0.8	Estimated
φ	The percentage of asymptomatic patients who progress to severely infected	5.00005E–2	50E–2	Estimated
ϵ	How quickly symptomatic individuals get well	8.05084E–2: 9.8026529E–2 day^{-1}	8.93E–2	[9]
α	Disease induced death rate	44E–2: 99E–2 day^{-1}	72E–2	Estimated

(Continued)

Table 1 (continued)

Parameter		Range	Baseline worth	Reference
m_1	How quickly asymptomatic patients discharge the pathogen into the surrounding environment	1.7804E–2 day^{-1}	1.78E–2	Estimated
m_2	The speed at which sick individuals discharge the infection into the surrounding area	92.152716E–2 day^{-1}	92.15E–2	Estimated
τ	The pace at which environmental viruses (Surfaces) naturally degrade	29E–2: 33.33E–2 day^{-1}	31.17E–2	[13]

In addition, we assume that all parameters are greater than zero and that compartment $I(t)$ is the one experiencing disease-induced death with a mean of a. The total infection strength was determined as $\lambda = S[\beta(\eta A + I) + \beta_1 V]$, where λ is the injury strength.

Moreover, the system assumes that no individual without symptoms transmits the infection.

Model (1) can be abbreviated to obtain total DE as follows:

$$\begin{cases} \dfrac{dG}{dt} = \Lambda - \omega G - \alpha I, \\ \dfrac{dV}{dt} = m_1 A + m_2 I - \tau V, \end{cases} \tag{3}$$

where $G(t)$ is the gross people of individuals.

Numerous classic and fractional models have been employed across various studies to examine the spread of COVID-19 [14,15]. These models enable us to predict regional epidemic peaks, assess the impact of different quarantine measures, and understand the transmission dynamics of COVID-19. The concept of fractional or incorrect order integration and differentiation can be traced back to the correct order computation configuration itself [16,17].

A mathematical theory suitable for exploring fractional calculus was developed over the years leading up to the nineteenth century.

However, the most significant advancements in engineering and scientific applications have occurred in the last century [18,19]. Calculation techniques in many situations meet the requirements of physical reality. Fractional order models have advantages over integer order models because such models incorporate a memory effect, which is important in biological processes [20,21].

Additionally, results obtained using the fractional technique are more generic in nature. Fractional differential equations (PDEs) have been used to study the majority of nonlinear issues that arise in

nature [22–25]. The benefit of FDE is that it has a non-local feature that exhibits the fresh features of these issues.

However, finding an exact solution to these kinds of issues is extremely hard. To find approximate solutions to most differential equations of fractional order, certain analytic techniques like perturbation techniques, symmetry techniques and others are feasible and usable [26,27]. It is obvious that one should realize that most of the techniques do not provide exact solutions to nonlinear differential equations.

Therefore, many analytical methods have been found that could find approximate solutions to such equations. The Temimi-Ansari method (TAM) is one of the most competitive in this field that Temimi and Ansari presented in 2011 [28–30] for solving differential equations, which were matched with computational approaches of previous studies, but only in their classical case.

In this paper, we will study the fractional order model of COVID-19 found in Ghana from 12 March 2020 to 07 May 2020 using two fractional derivatives, the Caputo fractional derivative [16] and ABC fractional derivative [31,32] which take the forms:

$$\begin{cases} {}^{C}D_t^{\sigma} S = \Lambda - \omega S - \beta\left[IS + \eta AS\right] - \beta_1 VS + \rho R, \\ {}^{C}D_t^{\sigma} E = \beta\left[IS + \eta AS\right] + \beta_1 VS - E\left\{k_2(1-\gamma) + k_1\gamma + \omega\right\}, \\ {}^{C}D_t^{\sigma} A = k_2(1-\gamma)E - A\left\{\omega + v_1\varphi + v_2(1-\varphi)\right\}, \\ {}^{C}D_t^{\sigma} I = k_1\gamma E + v_1\varphi A - I\left\{\epsilon + \omega + \alpha\right\}, \\ {}^{C}D_t^{\sigma} R = v_2(1-\varphi)A + \epsilon I - R(\rho + \omega), \\ {}^{C}D_t^{\sigma} V = m_1 A + m_2 I - \tau V, \end{cases} \tag{4}$$

and

$$\begin{cases} {}^{ABC}D_t^{\sigma} S = \Lambda - \omega S - \beta\left[IS + \eta AS\right] - \beta_1 VS + \rho R, \\ {}^{ABC}D_t^{\sigma} E = \beta\left[IS + \eta AS\right] + \beta_1 VS - E\left\{k_2(1-\gamma) + k_1\gamma + \omega\right\}, \\ {}^{ABC}D_t^{\sigma} A = k_2(1-\gamma)E - A\left\{\omega + v_1\varphi + v_2(1-\varphi)\right\}, \\ {}^{ABC}D_t^{\sigma} I = k_1\gamma E + v_1\varphi A - I\left\{\epsilon + \omega + \alpha\right\}, \\ {}^{ABC}D_t^{\sigma} R = v_2(1-\varphi)A + \epsilon I - R(\rho + \omega), \\ {}^{ABC}D_t^{\sigma} V = m_1 A + m_2 I - \tau V, \end{cases} \tag{5}$$

respectively.

The choice of the Caputo and Atangana-Baleanu fractional differential operators is motivated by their distinct advantages in capturing memory and hereditary properties of dynamical systems, which are crucial for accurately modeling the spread of infectious diseases like COVID-19. The Caputo operator is widely used in fractional calculus due to its compatibility with initial conditions defined in terms of integer-order derivatives, making it suitable for real-world applications where initial data is often provided in this form. However, the Caputo derivative has limitations in representing certain non-local effects.

In contrast, the Atangana-Baleanu fractional operator, defined in the Caputo sense (ABC), provides a more generalized framework by incorporating a non-singular kernel. This allows for a better description of complex systems with long-term memory and smoother transitions between states. By comparing the performance of both operators, we aim to determine which operator offers a more

accurate and realistic representation of the COVID-19 pandemic dynamics in Ghana, while exploring the differences in how each operator models memory effects.

The paper is arranged as follows: In Section 2, we offer a few essential definitions and ideas related to fractional calculus. In Section 3, we seek to study convergence analysis, and the existence of uniformly stable and unique solutions to the system by the Atangana Baleanu operator with Caputo Sense. In Section 4, we introduce the main concept of fractional Analytical technique (FTAM). In Section 5, we give a discussion of the results of this study. In the final section, conclusions are presented.

2 Basic Concepts and Definitions

In recent years, there have been several definitions of fractional calculus [16,17].

Definition 1. Assume that $\sigma > 0, \varrho > \varepsilon, \sigma, \varrho, \varepsilon \in \mathbb{R}$,

$$D_*^{\sigma}\varphi(\varrho) = I^{n-\sigma}D^{n}\varphi(\varrho) = \begin{cases} \dfrac{d^n}{d\varrho^n}\varphi(\varrho), & \sigma = n \in \mathbb{N}, \\ \dfrac{1}{\Gamma(n-\sigma)}\displaystyle\int_{\varepsilon}^{\varrho}(\varrho-\epsilon)^{n-\sigma-1}\varphi^{(n)}(\epsilon)\,d\epsilon, & n-1 < \sigma \le n \in \mathbb{N}. \end{cases} \tag{6}$$

where D_*^{σ} is the Caputo fractional differential operator of order σ.

Definition 2. The fractional integral operator of R-L of a function $\varphi(\varrho) \in C_t, t \ge -1$ is denoted by I_b^{σ} as

$$\begin{cases} I_b^{\sigma}\varphi(\varrho) &= \dfrac{1}{\Gamma(\sigma+1)}\displaystyle\int_b^{\varrho}\varphi(\varrho)(d\varrho)^{\sigma}, \\ &= \dfrac{1}{\Gamma(\sigma)}\displaystyle\int_b^{\varrho}(\varrho-\epsilon)^{\sigma-1}\varphi(\epsilon)\,d\epsilon, \quad \varrho,\sigma > 0, \\ I_b^{0}\varphi(\varrho) &= \varphi(\varrho). \end{cases} \tag{7}$$

Definition 3. The definition of Sobolev space $(\mathcal{S})$ in (e,f) of order 1 is defined as

$$\mathcal{S}^1(e,f) = \left\{\varphi \in L^2(e,f) : \varphi' \in L^2(e,f)\right\}. \tag{8}$$

Definition 4. If $\varphi \in \mathcal{S}^1(e,f), f > e, \sigma \in (0,1]$, then the definition of the AB fractional derivative in left Caputo sense (ABC) can be appeared by

$${}^{ABC}{}_{\varepsilon}D_{\varrho}^{\sigma}\varphi(\varrho) = \frac{AB(\sigma)}{1-\sigma}\int_{\varepsilon}^{\varrho}\varphi'(\varrho)E_{\sigma}\left[-\sigma\frac{(\varrho-\epsilon)^{\sigma}}{1-\sigma}\right]d\epsilon, \tag{9}$$

where $AB(\sigma)$ is a normalized function.

Definition 5. If $\varphi \in S^1(e,f), f > e, \sigma \in (0,1]$, consequently, the left Riemann-Liouville sense (ABR) definition of the AB fractional derivative can be shown by

$${}^{ABR}{}_{\varepsilon}D_{\varrho}^{\sigma}\varphi(\varrho) = \frac{AB(\sigma)}{1-\sigma}\left(\frac{d}{d\varrho}\right)\int_{\varepsilon}^{\varrho}\varphi(\varrho)E_{\sigma}\left[-\sigma\frac{(\varrho-\epsilon)^{\sigma}}{1-\sigma}\right]d\epsilon. \tag{10}$$

Definition 6. The fractional integral with non-local kernel which helper to the fractional derivative is defined as

$$
\begin{aligned}
{}^{AB}{}_{\varepsilon}I_{\varrho}^{\sigma}\varphi(\varrho) &= \frac{1-\sigma}{AB(\sigma)}\varphi(\varrho) + \frac{\sigma}{AB(\sigma)\Gamma(\sigma)}\int_{\varepsilon}^{\varrho}\varphi(\epsilon)(\varrho-\epsilon)^{\sigma-1}\,d\epsilon, \\
&= \frac{1-\sigma}{AB(\sigma)}\varphi(\varrho) + \frac{\sigma}{AB(\sigma)\Gamma(\sigma)}\left({}_{\varepsilon}I^{\sigma}\varphi(\varrho)\right). \qquad (11)
\end{aligned}
$$

If $\sigma = 0$, we recuperate the underlying function and if additionally $\sigma = 1$, we acquire the ordinary integral.

Definition 7. For any function $\varphi(t)$, the norm $\|\varphi(t)\|$ is defined as the supremum of the absolute value of $\varphi(t)$ over the domain $t \in [0, T]$, i.e.,

$$\|\varphi(t)\| = \sup\{|\varphi(t)| : t \in [0, T]\}. \qquad (12)$$

3 Convergence Analysis of the Model

3.1 Convergence Analysis

To provide the most effective affinity analysis for the technique discussed in this article, we will begin by detailing the subsequent steps of the presented analytical algorithm. We get the parts in these shapes

$$
\begin{cases}
\mu_0 = \omega_0(t), \\
\mu_1 = \Theta[\mu_0], \\
\mu_2 = \Theta[\mu_0 + \mu_1], \\
\vdots \\
\mu_{n+1} = \Theta[\mu_0 + \mu_1 + \cdots + \mu_n].
\end{cases} \qquad (13)
$$

The operator $\Theta[\omega(t)]$ can now be described as

$$\Theta[\mu_n] = \omega_n(t) - \sum_{i=0}^{n-1}\omega_i(t), \qquad n = 1, 2, 3, \cdots, \qquad (14)$$

where part $\omega_n(t)$ denotes the approximate solution that evidenced from the FTAM.

This approximate analytical method outlines the necessary stipulations for the convergence of the formula. The main findings are expressed in the following theories.

Theorem 1. *If $\omega(t) = \sum_{i=0}^{\infty}\omega_n(t)$ is convergent, it will illustrate the exact solution to the present issue.*

Proof 1. The sequence $\{G_n\}_{n=0}^{\infty}$ is defined as

$$
\begin{cases}
G_0 = \omega_0, \\
G_1 = \mu_0 + \mu_1, \\
G_2 = \mu_0 + \mu_1 + \mu_2, \\
\vdots \\
G_n = \mu_0 + \mu_1 + \cdots + \mu_n.
\end{cases} \qquad (15)
$$

In the Hilbert space H, we display that $\{G_n\}_{n=0}^{\infty}$ is a Cauchy sequence. Consider that

$$\|G_{n+1} - G_n\| = \|\mu_{n+1}\| \le \delta\|\mu_n\| \le \delta^2\|\mu_{n-1}\| \le \cdots \le \delta^{n+1}\|\mu_0\|. \qquad (16)$$

For every $n, j \in \mathbb{N}$, $n \geq j$, we have

$$\begin{aligned}\left\| G_n - G_j \right\| &= \left\| (G_n - G_{n-1}) + (G_{n-1} - G_{n-2}) + \cdots + \left(G_{j+1} - G_j\right) \right\| \\ &\leq \| (G_n - G_{n-1}) \| + \| (G_{n-1} - G_{n-2}) \| + \cdots + \left\| \left(G_{j+1} - G_j\right) \right\| \\ &\leq \delta^n \| \mu_0 \| + \delta^{n-1} \| \mu_0 \| + \cdots + \delta^{j+1} \| \mu_0 \| = \frac{1 - \delta^{n-j}}{1 - \delta} \delta^{j+1} \| \mu_0 \| , \end{aligned} \tag{17}$$

and since $0 < \delta < 1$, we get

$$\lim_{n,j \Longrightarrow \infty} \left\| G_n - G_j \right\| = 0. \tag{18}$$

As a result, $\{G_n\}_{n=0}^{\infty}$ is a Cauchy sequence in the Hilbert space H, implying that the series solution $\omega(t) = \sum_{i=0}^{n} \mu_n(t)$ converges. This proof is complete. □

Theorem 2. *Assume that* Θ *defined in Eq. (14), is an operator that goes from the Hilbert space* $\mathcal{H}$ *to* $\mathcal{H}$.

The series solution $\omega(t) = \sum_{i=0}^{n} \omega_n(t)$ *converges if* $\exists\ 0 < \delta < 1$ *such that*

$\| \Theta [\mu_0 + \mu_1 + \cdots + \mu_{n+1}] \| \leq \delta \| \Theta [\mu_0 + \mu_1 + \cdots + \mu_n] \|$ (*such that* $\| \mu_{n+1} \| \leq \delta \| \mu_n \|$) $\forall \delta \in \mathbb{N} \cup \{0\}$.

When we look at the fixed point principle more closely, we see that the antecedent theory is a private case of it and that it is deemed a necessary condition for discussing the FTAM's convergence [33].

Theorem 3. *Assume that the series solution* $\sum_{i=0}^{\infty} \omega_n(t)$ *be convergent to* $\omega(t)$, *the maximum error* $E_n(t)$ *is evaluated by*

$$E_n(\chi, \tau) \leq \frac{1}{1 - \delta} \delta^{n+1} \| \omega_0 \| , \tag{19}$$

if the amputated series $\sum_{i=0}^{n} \omega_i(t)$ *is utilized as an approach to the solution of the present nonlinear issue [33].*

Briefly, Theorems 1 and 2 express that FTAM for linear and nonlinear issues, was obtained utilizing the analytical iteration Eqs. (13) or (74), converges to an exact solution if $\| \Theta [\mu_0 + \mu_1 + \cdots + \mu_{n+1}] \| \leq \delta \| \Theta [\mu_0 + \mu_1 + \cdots + \mu_n] \|$ (that is $\| \mu_{n+1} \| \leq \delta \| \mu_n \|$) $\forall \delta \in \mathbb{N} \cup \{0\}$ under the condition that $\exists\ 0 < \delta < 1$. TAM's solution converges to the exact solution, according to the theoretical description under the condition: $\exists 0 < \delta < 1$ such that

$$C_n = \begin{cases} \dfrac{\| \mu_{n+1} \|}{\| \mu_n \|}, & \| \mu_n \| \neq 0, \\ 0, & \| \mu_n \| = 0, \end{cases} \tag{20}$$

when $0 \leq C_n < 1$, $\forall n = 0, 1, 2, \cdots$, then, the solution $\sum_{n=0}^{\infty} \omega_n(t)$ converges to $\omega(t)$.

3.2 *Existence of Uniformly Stable Solution*

Suppose that

$$\begin{cases} D_t^\sigma S = \Lambda - \omega S - \beta\left[IS + \eta AS\right] - \beta_1 VS + \rho R \\ \qquad = Y_1\left(S, E, A, I, R, t\right), \\ D_t^\sigma E = \beta\left[IS + \eta AS\right] + \beta_1 VS - E\left\{k_2(1-\gamma) + k_1\gamma + \omega\right\} \\ \qquad = Y_2\left(S, E, A, I, R, t\right), \\ D_t^\sigma A = k_2(1-\gamma)E - A\left\{\omega + v_1\varphi + v_2(1-\varphi)\right\} \\ \qquad = Y_3\left(S, E, A, I, R, t\right), \\ D_t^\sigma I = k_1\gamma E + v_1\varphi A - I\left\{\epsilon + \omega + \alpha\right\} \\ \qquad = Y_4\left(S, E, A, I, R, t\right), \\ D_t^\sigma R = v_2(1-\varphi)A + \epsilon I - R(\rho + \omega) \\ \qquad = Y_5\left(S, E, A, I, R, t\right), \\ D_t^\sigma V = m_1 A + m_2 I - \tau V \\ \qquad = Y_6\left(S, E, A, I, R, t\right). \end{cases} \tag{21}$$

For a constant $\mathcal{N}$, suppose that

$$\Theta = \left\{(S(t), E(t), A(t), I(t), R(t), V(t)) \in \mathbb{R}^6 : |X(t)| \leq \mathcal{N}, 0 \leq t \leq t\right\}. \tag{22}$$

At that point over, we get

$$\frac{\partial Y_1}{\partial S} = -\omega - \beta\left[I + \eta A\right] - \beta_1 V \Longrightarrow \left|\frac{\partial Y_1}{\partial S}\right| = \omega + \beta\left[I + \eta A\right] + \beta_1 V \leq h_{11}; \frac{\partial Y_1}{\partial E} = 0 \Longrightarrow Y_1\left(E\right) = h_{12};$$

$$\frac{\partial Y_1}{\partial A} = -\beta\eta S \Longrightarrow \left|\frac{\partial Y_1}{\partial A}\right| = \beta\eta S \leq h_{13}; \frac{\partial Y_1}{\partial I} = -\beta S \Longrightarrow \left|\frac{\partial Y_1}{\partial I}\right| = \beta S \leq h_{14}; \tag{23}$$

$$\frac{\partial Y_1}{\partial R} = \rho \Longrightarrow \left|\frac{\partial Y_1}{\partial R}\right| = \rho \leq h_{15}; \frac{\partial Y_1}{\partial V} = -\beta_1 V \Longrightarrow \left|\frac{\partial Y_1}{\partial V}\right| = \beta_1 V \leq h_{16};$$

$$\frac{\partial Y_2}{\partial S} = \beta\left[I + \eta A\right] + \beta_1 V \Longrightarrow \left|\frac{\partial Y_2}{\partial S}\right| = \beta\left[I + \eta A\right] + \beta_1 V \leq h_{21};$$

$$\frac{\partial Y_2}{\partial E} = -\left\{k_2(1-\gamma) + k_1\gamma + \omega\right\} \Longrightarrow \left|\frac{\partial Y_2}{\partial E}\right| = k_2(1-\gamma) + k_1\gamma + \omega \leq h_{22}; \frac{\partial Y_2}{\partial A} = \beta\eta S \Longrightarrow \left|\frac{\partial Y_2}{\partial A}\right|$$
$$= \beta\eta S \leq h_{23}; \tag{24}$$

$$\frac{\partial Y_2}{\partial I} = \beta S \Longrightarrow \left|\frac{\partial Y_2}{\partial I}\right| = \beta S \leq h_{24}; \frac{\partial Y_2}{\partial R} = 0 \Longrightarrow Y_2\left(R\right) = h_{25}; \frac{\partial Y_2}{\partial V} = \beta_1 S \Longrightarrow \left|\frac{\partial Y_2}{\partial V}\right| = \beta_1 S \leq h_{26};$$

$$\frac{\partial Y_3}{\partial S} = 0 \Longrightarrow Y_3(S) = h_{31}; \frac{\partial Y_3}{\partial E} = k_2(1-\gamma) \Longrightarrow \left|\frac{\partial Y_3}{\partial E}\right| = k_2(1-\gamma) \leq h_{32};$$

$$\frac{\partial Y_3}{\partial A} = -\{\omega + v_1\varphi + v_2(1-\varphi)\} \Longrightarrow \left|\frac{\partial Y_3}{\partial A}\right| = \omega + v_1\varphi + v_2(1-\varphi) \leq h_{33}; \frac{\partial Y_3}{\partial I} = 0 \Longrightarrow Y_3(I) = h_{34}; \quad (25)$$

$$\frac{\partial Y_3}{\partial R} = 0 \Longrightarrow Y_3(R) = h_{35}; \frac{\partial Y_3}{\partial V} = 0 \Longrightarrow Y_3(V) = h_{36};$$

$$\frac{\partial Y_4}{\partial S} = 0 \Longrightarrow Y_4(S) = h_{41}; \frac{\partial Y_4}{\partial E} = k_1\gamma \Longrightarrow \left|\frac{\partial Y_4}{\partial E}\right| = k_1\gamma \leq h_{42}; \frac{\partial Y_4}{\partial A} = v_1\varphi \Longrightarrow \left|\frac{\partial Y_4}{\partial A}\right| = v_1\varphi \leq h_{43};$$

$$\frac{\partial Y_4}{\partial I} = -\{\epsilon + \omega + \alpha\} \Longrightarrow \left|\frac{\partial Y_4}{\partial A}\right| = \epsilon + \omega + \alpha \leq h_{44}; \frac{\partial Y_4}{\partial R} = 0 \Longrightarrow Y_4(R) = h_{45};$$

$$\frac{\partial Y_4}{\partial V} = 0 \Longrightarrow Y_4(V) = h_{46}; \quad (26)$$

$$\frac{\partial Y_5}{\partial S} = 0 \Longrightarrow Y_5(S) = h_{51}; \frac{\partial Y_5}{\partial E} = 0 \Longrightarrow Y_5(E) = h_{52}; \frac{\partial Y_5}{\partial A} = v_2(1-\varphi) \Longrightarrow \left|\frac{\partial Y_5}{\partial A}\right| = v_2(1-\varphi) \leq h_{53};$$

$$\frac{\partial Y_5}{\partial I} = \epsilon \Longrightarrow \left|\frac{\partial Y_5}{\partial A}\right| = \epsilon \leq h_{54}; \frac{\partial Y_5}{\partial R} = -(\rho + \omega) \Longrightarrow \left|\frac{\partial Y_5}{\partial R}\right| = \rho + \omega \leq h_{55}; \frac{\partial Y_5}{\partial V} = 0 \Longrightarrow Y_5(V) = h_{56}; \quad (27)$$

$$\frac{\partial Y_6}{\partial S} = 0 \Longrightarrow Y_6(S) = h_{61}; \frac{\partial Y_6}{\partial E} = 0 \Longrightarrow Y_6(E) = h_{62}; \frac{\partial Y_6}{\partial A} = m_1 \Longrightarrow \left|\frac{\partial Y_6}{\partial A}\right| = m_1 \leq h_{63};$$

$$\frac{\partial Y_6}{\partial I} = m_2 \Longrightarrow \left|\frac{\partial Y_6}{\partial A}\right| = m_2 \leq h_{64}; \frac{\partial Y_6}{\partial R} = 0 \Longrightarrow Y_6(R) = h_{65}; \frac{\partial Y_6}{\partial V} = -\sigma \Longrightarrow \left|\frac{\partial Y_6}{\partial V}\right| = \tau \leq h_{66}; \quad (28)$$

where $h_{yz} > 0$ and $1 \leq y, z \leq 6$.

From the foregoing, we conclude that the Lipschitz condition is valid in each of the functions from (23) to (28).

In the next part, we will prove the existence of solutions of the model (5). Let $\sigma = \Upsilon(\lambda) \times (\lambda)$ and $\Upsilon(\lambda)$ be a Banach space on λ with the norm

$$\|S, E, A, I, R, V\| = \|S\| + \|E\| + \|A\| + \|I\| + \|R\| + \|V\|,$$

where

$$\begin{cases} \|S\| = sup\{|S(t)| : t \in \lambda\}, \\ \|E\| = sup\{|E(t)| : t \in \lambda\}, \\ \|A\| = sup\{|A(t)| : t \in \lambda\}, \\ \|I\| = sup\{|I(t)| : t \in \lambda\}, \\ \|R\| = sup\{|R(t)| : t \in \lambda\}, \\ \|V\| = sup\{|V(t)| : t \in \lambda\}. \end{cases} \tag{29}$$

We can transform Eq. (5) to a Volterra type integral equation as

$$S(t) - S(0) = \frac{1-\sigma}{AB(\sigma)}\{\Lambda - \omega S(t) - \beta[I(t)S(t) + \eta A(t)S(t)] - \beta_1 V(t)S(t) + \rho R(t)\} + \frac{\sigma}{AB(\sigma)\Gamma(\sigma)} \times \int_0^t (t-\varrho)^{\sigma-1}\{\Lambda - \omega S(\varrho) - \beta[I(\varrho)S(\varrho) + \eta A(\varrho)S(\varrho)] - \beta_1 V(\varrho)S(\varrho) + \rho R(\varrho)\}\, d\varrho, \tag{30}$$

$$E(t) - E(0) = \frac{1-\sigma}{AB(\sigma)}\{\beta[I(t)S(t) + \eta A(t)S(t)] + \beta_1 V(t)S(t) - E(t)\{k_2(1-\gamma) + k_1\gamma + \omega\}\} + \frac{\sigma}{AB(\sigma)\Gamma(\sigma)} \times \int_0^t (t-\varrho)^{\sigma-1}\{\beta[I(\varrho)S(\varrho) + \eta A(\varrho)S(\varrho)] + \beta_1 V(\varrho)S(\varrho) - E(\varrho)\{k_2(1-\gamma) + k_1\gamma + \omega\}\}\, d\varrho, \tag{31}$$

$$A(t) - A(0) = \frac{1-\sigma}{AB(\sigma)}\{k_2(1-\gamma)E(t) - A(t)\{\omega + v_1\varphi + v_2(1-\varphi)\}\} + \frac{\sigma}{AB(\sigma)\Gamma(\sigma)} \times \int_0^t (t-\varrho)^{\sigma-1}\{k_2(1-\gamma)E(\varrho) - A(\varrho)\{\omega + v_1\varphi + v_2(1-\varphi)\}\}\, d\varrho, \tag{32}$$

$$I(t) - I(0) = \frac{1-\sigma}{AB(\sigma)}\{k_1\gamma E(t) + v_1\varphi A(t) - I(t)\{\epsilon + \omega + \alpha\}\} + \frac{\sigma}{AB(\sigma)\Gamma(\sigma)} \times \int_0^t (t-\varrho)^{\sigma-1}\{k_1\gamma E(\varrho) + v_1\varphi A(\varrho) - I(\varrho)\{\epsilon + \omega + \alpha\}\}\, d\varrho, \tag{33}$$

$$R(t) - R(0) = \frac{1-\sigma}{AB(\sigma)}\{v_2(1-\varphi)A(t) + \epsilon I(t) - R(t)(\rho + \omega)\} + \frac{\sigma}{AB(\sigma)\Gamma(\sigma)} \times \int_0^t (t-\varrho)^{\sigma-1}\{v_2(1-\varphi)A(\varrho) + \epsilon I(\varrho) - R(\varrho)(\rho + \omega)\}\, d\varrho, \tag{34}$$

$$V(t) - V(0) = \frac{1-\sigma}{AB(\sigma)}\{m_1 A(t) + m_2 I(t) - \sigma V(t)\} + \frac{\sigma}{AB(\sigma)\Gamma(\sigma)} \times \int_0^t (t-\varrho)^{\sigma-1}\{m_1 A(\varrho) + m_2 I(\varrho) - \tau V(\varrho)\}\, d\varrho. \tag{35}$$

Suppose for simplicity

$$\begin{cases} \Upsilon_1(t,S) = \Lambda - \omega S - \beta[IS + \eta AS] - \beta_1 VS + \rho R, \\ \Upsilon_2(t,E) = \beta[IS + \eta AS] + \beta_1 VS - E\{k_2(1-\gamma) + k_1\gamma + \omega\}, \\ \Upsilon_3(t,A) = k_2(1-\gamma)E - A\{\omega + v_1\varphi + v_2(1-\varphi)\}, \\ \Upsilon_4(t,I) = k_1\gamma E + v_1\varphi A - I\{\epsilon + \omega + \alpha\}, \\ \Upsilon_5(t,R) = v_2(1-\varphi)A + \epsilon I - R(\rho + \omega), \\ \Upsilon_6(t,V) = m_1 A + m_2 I - \tau V. \end{cases} \tag{36}$$

Theorem 4. *The Lipschitz condition is satisfied by the kernels Eq. (36)* Υ_i, $i = 1, 2, \cdots, 6$, *if the next inequality holds:* $0 \le \chi_i < 1,\ i = 1, 2, \cdots, 6$.

Proof 2. We start by analyzing the kernel $\Upsilon_1(t,S)$. Consider two functions, S and S^*, in which

$$\begin{aligned} \left\|\Upsilon_1(t,S) - \Upsilon_1(t,S^*)\right\| &= \|(\omega + \beta[I + \eta A] + \beta_1 V)(S(t) - S^*(t))\| \\ &\le (\omega + \beta[\|I\| + \eta\|A\|] + \beta_1\|V\|)\|S(t) - S^*(t)\| \le \chi_1\left\|S(t) - S^*(t)\right\|, \end{aligned} \tag{37}$$

Similarly, for the other kernels, we have

$$\|\Upsilon_2(t,E) - \Upsilon_2(t,E^*)\| \le \chi_2\|E(t) - E^*(t)\|, \tag{38}$$

$$\|\Upsilon_3(t,A) - \Upsilon_3(t,A^*)\| \le \chi_3\|A(t) - A^*(t)\|, \tag{39}$$

$$\|\Upsilon_4(t,I) - \Upsilon_4(t,I^*)\| \le \chi_4\|I(t) - I^*(t)\|, \tag{40}$$

$$\|\Upsilon_5(t,R) - \Upsilon_5(t,R^*)\| \le \chi_5\|R(t) - R^*(t)\|, \tag{41}$$

$$\|\Upsilon_6(t,V) - \Upsilon_6(t,V^*)\| \le \chi_6\|V(t) - V^*(t)\|, \tag{42}$$

where $a = \max_{t\in A(t)} \|A(t)\|, i = \max_{t\in I(t)} \|I(t)\|, v = \max_{t\in V(t)} \|V(t)\|$ and

$$\begin{cases} \chi_1 = \omega + \beta\,[i + \eta a] + \beta_1 v, \\ \chi_2 = k_2(1-\gamma) + k_1\gamma + \omega, \\ \chi_3 = \omega + v_1\varphi + v_2(1-\varphi), \\ \chi_4 = \epsilon + \omega + \alpha, \\ \chi_5 = \rho + \omega, \\ \chi_6 = \tau. \end{cases} \tag{43}$$

The following can be used to represent the kernels of the model (5):

$$\begin{cases} S(t) = S(0) + \frac{1-\sigma}{AB(\sigma)}\Upsilon_1(t,S) + \frac{\sigma}{AB(\sigma)\Gamma(\sigma)}\int_0^t (t-\varrho)^{\sigma-1}\Upsilon_1(\varrho,S)d\varrho, \\ E(t) = E(0) + \frac{1-\sigma}{AB(\sigma)}\Upsilon_2(t,E) + \frac{\sigma}{AB(\sigma)\Gamma(\sigma)}\int_0^t (t-\varrho)^{\sigma-1}\Upsilon_2(\varrho,E)d\varrho, \\ A(t) = A(0) + \frac{1-\sigma}{AB(\sigma)}\Upsilon_3(t,A) + \frac{\sigma}{AB(\sigma)\Gamma(\sigma)}\int_0^t (t-\varrho)^{\sigma-1}\Upsilon_3(\varrho,A)d\varrho, \\ I(t) = I(0) + \frac{1-\sigma}{AB(\sigma)}\Upsilon_4(t,I) + \frac{\sigma}{AB(\sigma)\Gamma(\sigma)}\int_0^t (t-\varrho)^{\sigma-1}\Upsilon_4(\varrho,I)d\varrho, \\ R(t) = R(0) + \frac{1-\sigma}{AB(\sigma)}\Upsilon_5(t,R) + \frac{\sigma}{AB(\sigma)\Gamma(\sigma)}\int_0^t (t-\varrho)^{\sigma-1}\Upsilon_5(\varrho,R)d\varrho, \\ V(t) = V(0) + \frac{1-\sigma}{AB(\sigma)}\Upsilon_6(t,V) + \frac{\sigma}{AB(\sigma)\Gamma(\sigma)}\int_0^t (t-\varrho)^{\sigma-1}\Upsilon_6(\varrho,V)d\varrho. \end{cases} \tag{44}$$

Consider the next iterative formula and initial conditions as

$$\begin{cases} S_n(t) = S(0) + \frac{1-\sigma}{AB(\sigma)}\Upsilon_1(t,S_{n-1}) + \frac{\sigma}{AB(\sigma)\Gamma(\sigma)}\int_0^t (t-\varrho)^{\sigma-1}\Upsilon_1(\varrho,S_{n-1})d\varrho, \\ E_n(t) = E(0) + \frac{1-\sigma}{AB(\sigma)}\Upsilon_2(t,E_{n-1}) + \frac{\sigma}{AB(\sigma)\Gamma(\sigma)}\int_0^t (t-\varrho)^{\sigma-1}\Upsilon_2(\varrho,E_{n-1})d\varrho, \\ A_n(t) = A(0) + \frac{1-\sigma}{AB(\sigma)}\Upsilon_3(t,A_{n-1}) + \frac{\sigma}{AB(\sigma)\Gamma(\sigma)}\int_0^t (t-\varrho)^{\sigma-1}\Upsilon_3(\varrho,A_{n-1})d\varrho, \\ I_n(t) = I(0) + \frac{1-\sigma}{AB(\sigma)}\Upsilon_4(t,I_{n-1}) + \frac{\sigma}{AB(\sigma)\Gamma(\sigma)}\int_0^t (t-\varrho)^{\sigma-1}\Upsilon_4(\varrho,I_{n-1})d\varrho, \\ R_n(t) = R(0) + \frac{1-\sigma}{AB(\sigma)}\Upsilon_5(t,R_{n-1}) + \frac{\sigma}{AB(\sigma)\Gamma(\sigma)}\int_0^t (t-\varrho)^{\sigma-1}\Upsilon_5(\varrho,R_{n-1})d\varrho, \\ V_n(t) = V(0) + \frac{1-\sigma}{AB(\sigma)}\Upsilon_6(t,V_{n-1}) + \frac{\sigma}{AB(\sigma)\Gamma(\sigma)}\int_0^t (t-\varrho)^{\sigma-1}\Upsilon_6(\varrho,V_{n-1})d\varrho, \end{cases} \tag{45}$$

and $S(0) \geq 0, E(0) \geq 0, A(0) \geq 0, I(0) \geq 0, R(0) \geq 0, V(0) \geq 0$, respectively.

The variance between the successive components assumes the following form:

$$\mathcal{S}(t) = S_n(t) - S_{n-1}(t) = \frac{1-\sigma}{AB(\sigma)}\left[\Upsilon_1(t, S_{n-1}) - \Upsilon_1(t, S_{n-2})\right] + \frac{\sigma}{AB(\sigma)\Gamma(\sigma)} \times \int_0^t (t-\varrho)^{\sigma-1}\left[\Upsilon_1(\varrho, S_{n-1}) - \Upsilon_1(\varrho, S_{n-2})\right] d\varrho, \tag{46}$$

$$\mathcal{E}(t) = E_n(t) - E_{n-1}(t) = \frac{1-\sigma}{AB(\sigma)}\left[\Upsilon_2(t, E_{n-1}) - \Upsilon_2(t, E_{n-2})\right] + \frac{\sigma}{AB(\sigma)\Gamma(\sigma)} \times \int_0^t (t-\varrho)^{\sigma-1}\left[\Upsilon_2(\varrho, E_{n-1}) - \Upsilon_2(\varrho, E_{n-2})\right] d\varrho, \tag{47}$$

$$\mathcal{A}(t) = A_n(t) - A_{n-1}(t) = \frac{1-\sigma}{AB(\sigma)}\left[\Upsilon_3(t, A_{n-1}) - \Upsilon_3(t, A_{n-2})\right] + \frac{\sigma}{AB(\sigma)\Gamma(\sigma)} \times \int_0^t (t-\varrho)^{\sigma-1}\left[\Upsilon_3(\varrho, A_{n-1}) - \Upsilon_3(\varrho, A_{n-2})\right] d\varrho, \tag{48}$$

$$\mathcal{I}(t) = I_n(t) - I_{n-1}(t) = \frac{1-\sigma}{AB(\sigma)}\left[\Upsilon_4(t, I_{n-1}) - \Upsilon_4(t, I_{n-2})\right] + \frac{\sigma}{AB(\sigma)\Gamma(\sigma)} \times \int_0^t (t-\varrho)^{\sigma-1}\left[\Upsilon_4(\varrho, I_{n-1}) - \Upsilon_4(\varrho, I_{n-2})\right] d\varrho, \tag{49}$$

$$\mathcal{R}(t) = R_n(t) - R_{n-1}(t) = \frac{1-\sigma}{AB(\sigma)}\left[\Upsilon_5(t, R_{n-1}) - \Upsilon_5(t, R_{n-2})\right] + \frac{\sigma}{AB(\sigma)\Gamma(\sigma)} \times \int_0^t (t-\varrho)^{\sigma-1}\left[\Upsilon_5(\varrho, R_{n-1}) - \Upsilon_5(\varrho, R_{n-2})\right] d\varrho, \tag{50}$$

$$\mathcal{V}(t) = V_n(t) - V_{n-1}(t) = \frac{1-\sigma}{AB(\sigma)}\left[\Upsilon_6(t, V_{n-1}) - \Upsilon_6(t, V_{n-2})\right] + \frac{\sigma}{AB(\sigma)\Gamma(\sigma)} \times \int_0^t (t-\varrho)^{\sigma-1}\left[\Upsilon_6(\varrho, V_{n-1}) - \Upsilon_6(\varrho, V_{n-2})\right] d\varrho. \tag{51}$$

From the above equations and calculations, one may see that

$$S_n(t)=\sum_{i=0}^{n}\mathcal{S}_i(t),\quad E_n(t)=\sum_{i=0}^{n}\mathcal{E}_i(t),\quad A_n(t)=\sum_{i=0}^{n}\mathcal{A}_i(t),\quad I_n(t)=\sum_{i=0}^{n}\mathcal{I}_i(t),\quad R_n(t)=\sum_{i=0}^{n}\mathcal{R}_i(t),$$

$$V_n(t)=\sum_{i=0}^{n}\mathcal{V}_i(t). \tag{52}$$

By applying the norm property on Susceptible (S) of Eq. (46), we get

$$\begin{aligned}\|\mathcal{S}(t)\| &= \|S_n(t)-S_{n-1}(t)\|\\ &\le \frac{1-\sigma}{AB(\sigma)}\|\Upsilon_1(t,S_{n-1})-\Upsilon_1(t,S_{n-2})\|+\frac{\sigma}{AB(\sigma)\Gamma(\sigma)}\int_0^t(t-\varrho)^{\sigma-1}\|\Upsilon_1(\varrho,S_{n-1})-\Upsilon_1(\varrho,S_{n-2})\|d\varrho.\end{aligned} \tag{53}$$

Since the Lipschitz condition is fulfilled in the kernels, we get

$$\|S_{n-1}(t)-S_{n-2}(t)\|\le\frac{1-\sigma}{AB(\sigma)}\chi_1\|S_{n-1}(t)-S_{n-2}(t)\|+\frac{\sigma}{AB(\sigma)\Gamma(\sigma)}\chi_1\int_0^t(t-\varrho)^{\sigma-1}\|S_{n-1}(\varrho)-S_{n-2}(\varrho)\|d\varrho, \tag{54}$$

then we have

$$\|\mathcal{S}_n(t)\|\le\frac{1-\sigma}{AB(\sigma)}\chi_1\|S_{n-1}(t)-S_{n-2}(t)\|+\frac{\sigma}{AB(\sigma)\Gamma(\sigma)}\chi_1\int_0^t(t-\varrho)^{\sigma-1}\|S_{n-1}(\varrho)-S_{n-2}(\varrho)\|d\varrho, \tag{55}$$

Likewise for Eqs. (47)–(51), we get the next

$$\|\mathcal{E}_n(t)\|\le\frac{1-\sigma}{AB(\sigma)}\chi_2\|E_{n-1}(t)-E_{n-2}(t)\|+\frac{\sigma}{AB(\sigma)\Gamma(\sigma)}\chi_2\int_0^t(t-\varrho)^{\sigma-1}\|E_{n-1}(\varrho)-E_{n-2}(\varrho)\|d\varrho, \tag{56}$$

$$\|\mathcal{A}_n(t)\|\le\frac{1-\sigma}{AB(\sigma)}\chi_3\|A_{n-1}(t)-A_{n-2}(t)\|+\frac{\sigma}{AB(\sigma)\Gamma(\sigma)}\chi_3\int_0^t(t-\varrho)^{\sigma-1}\|A_{n-1}(\varrho)-A_{n-2}(\varrho)\|d\varrho, \tag{57}$$

$$\|\mathcal{I}_n(t)\|\le\frac{1-\sigma}{AB(\sigma)}\chi_4\|I_{n-1}(t)-I_{n-2}(t)\|+\frac{\sigma}{AB(\sigma)\Gamma(\sigma)}\chi_4\int_0^t(t-\varrho)^{\sigma-1}\|I_{n-1}(\varrho)-I_{n-2}(\varrho)\|d\varrho, \tag{58}$$

$$\|\mathcal{R}_n(t)\|\le\frac{1-\sigma}{AB(\sigma)}\chi_5\|R_{n-1}(t)-R_{n-2}(t)\|+\frac{\sigma}{AB(\sigma)\Gamma(\sigma)}\chi_5\int_0^t(t-\varrho)^{\sigma-1}\|R_{n-1}(\varrho)-R_{n-2}(\varrho)\|d\varrho, \tag{59}$$

$$\left\|\mathcal{V}_n(t)\right\| \leq \frac{1-\sigma}{AB(\sigma)}\chi_6\left\|V_{n-1}(t)-V_{n-2}(t)\right\| + \frac{\sigma}{AB(\sigma)\Gamma(\sigma)}\chi_6\int_0^t (t-\varrho)^{\sigma-1}\left\|V_{n-1}(\varrho)-V_{n-2}(\varrho)\right\|d\varrho. \tag{60}$$

3.3 Uniqueness of Solutions

For the first model Eq. (5), we find that

$$S(t)-S^*(t) = \frac{1-\sigma}{AB(\sigma)}\left(\Upsilon_1(t,S)-\Upsilon_1(t,S^*)\right) + \frac{\sigma}{AB(\sigma)\Gamma(\sigma)}\int_0^t (t-\varrho)^{\sigma-1}\left(\Upsilon_1(t,S)-\Upsilon_1(t,S^*)\right)d\varrho. \tag{61}$$

From applying norm on above equations, we get

$$\left\|S(t)-S^*(t)\right\| \leq \frac{1-\sigma}{AB(\sigma)}\left\|\Upsilon_1(t,S)-\Upsilon_1(t,S^*)\right\| + \frac{\sigma}{AB(\sigma)\Gamma(\sigma)}\int_0^t (t-\varrho)^{\sigma-1}\left\|\Upsilon_1(\varrho,S)-\Upsilon_1(\varrho,S^*)\right\|d\varrho. \tag{62}$$

In this way, we get

$$\left\|S(t)-S^*(t)\right\| \leq \frac{1-\sigma}{AB(\sigma)}\chi_1\left\|S(t)-S^*(t)\right\| + \frac{\chi_1 t^\sigma}{AB(\sigma)\Gamma(\sigma)}\left\|S(t)-S^*(t)\right\|. \tag{63}$$

Then, we find that

$$\left\|S(t)-S^*(t)\right\|\left(1-\frac{1-\sigma}{AB(\sigma)}\chi_1-\frac{\chi_1 t^\sigma}{AB(\sigma)\Gamma(\sigma)}\right) \leq 0, \tag{64}$$

$$\left\|S(t)-S^*(t)\right\| = 0 \Longrightarrow S(t) = S^*(t).$$

From this evidence, we can use the same approach to demonstrate the uniqueness of the solutions to functions $E(t)$, $A(t)$, $I(t)$ $R(t)$ and $V(t)$.

3.4 Sensibility Analysis of Reproduction Number ($\mathcal{R}_0$) Without Control

So as to investigate the sensibility of $\mathcal{R}_0$ to every one of its components, we locate the partial derivative for every parameter in the reproduction number $\mathcal{R}_0$.

$$\begin{aligned}
\frac{\partial\mathcal{R}_0}{\partial\Lambda} &= \frac{\beta_1\left(m_2\left(\gamma C k_1+v_1 X\phi\right)+m_1 Q\right)+\beta\varrho\left(\gamma C k_1+\rho v_1 X+tXY\right)}{C\varrho t\omega Y} > 0,\\
\frac{\partial\mathcal{R}_0}{\partial\beta} &= \frac{\Lambda\left(\gamma C k_1+\rho v_1 X+tXY\right)}{Ct\omega Y} > 0,
\end{aligned} \tag{65}$$

$$\begin{aligned}
\frac{\partial\mathcal{R}_0}{\partial\omega} &= -\frac{\Lambda\left(\beta_1\left(m_2\left(\gamma C k_1+v_1 X\phi\right)+m_1 Q\right)+\beta\varrho\left(\gamma C k_1+\rho v_1 X+tXY\right)\right)}{C\varrho t\omega^2 Y} < 0,\\
\frac{\partial\mathcal{R}_0}{\partial k_1} &= \frac{\gamma\Lambda\left(\beta\varrho+\beta_1 m_2\right)}{\varrho t\omega Y} > 0,
\end{aligned} \tag{66}$$

$$\frac{\partial \mathcal{R}_0}{\partial \gamma} = \frac{k_1 \Lambda \left(\beta \varrho + \beta_1 m_2\right)}{\varrho t \omega Y} > 0, \quad \frac{\partial \mathcal{R}_0}{\partial \rho} = \frac{\Lambda X \left(\beta \rho \varrho + \beta_1 m_2 \phi\right)}{C \varrho t \omega Y} > 0,$$
$$\frac{\partial \mathcal{R}_0}{\partial \beta_1} = \frac{\Lambda \left(m_2 \left(\gamma C k_1 + v_1 X \phi\right) + m_1 Q\right)}{C \varrho t \omega Y} > 0, \tag{67}$$

$$\frac{\partial \mathcal{R}_0}{\partial \varrho} = -\frac{\beta_1 \Lambda \left(m_2 \left(\gamma C k_1 + v_1 X \phi\right) + m_1 Q\right)}{C \varrho^2 t \omega Y} < 0, \quad \frac{\partial \mathcal{R}_0}{\partial m_2} = \frac{\beta_1 \Lambda \left(\gamma C k_1 + v_1 X \phi\right)}{C \varrho t \omega Y} > 0, \quad \frac{\partial \mathcal{R}_0}{\partial t} = \frac{\beta \Lambda X}{C t \omega} > 0, \tag{68}$$

$$\frac{\partial \mathcal{R}_0}{\partial v_1} = \frac{\Lambda X \left(\beta \rho \varrho + \beta_1 m_2 \phi\right)}{C \varrho t \omega Y} > 0, \quad \frac{\partial \mathcal{R}_0}{\partial m_1} = \frac{\beta_1 \Lambda Q}{C \varrho t \omega Y} > 0, \quad \frac{\partial \mathcal{R}_0}{\partial \varphi} = \frac{\beta_1 \Lambda m_2 v_1 X}{C \varrho t \omega Y} > 0. \tag{69}$$

In sensitivity analysis, it was determined that $\mathcal{R}_0$ increases with all parameters in $\mathcal{R}_0$ except for two parameters and decreases with ω and ϱ.

This means that to reduce disease prevalence, those parameters with negative rates of the fractional derivative must be reduced in the environment. Since the $\mathcal{R}_0$ value is equal to 2.68 without control reserves in Ghana based on what has been calculated, this shows, on average, that one infectious person can spread the disease from 2 to 3 susceptible people [10].

Therefore, encouraging preventive measures including social distancing, using nasal masks, routinely washing hands with disinfectant, and reducing contact will disrupt the primary mechanisms that facilitate the disease's spread.

4 Numerical Simulation

In this section, we examine the novel coronavirus known as the SEAIRV model with Caputo and ABC fractional derivatives to display our algorithm's potential, spread, and superiority. All analytic and numerical calculations were completed using the MATHEMATICA 12 software package during the computation time.

4.1 The Main Idea for TAM of Fractional Order

The general non-homogeneous fractional differential equation (FDE) is used to explain the basic ideas of the suggested algorithm as [28,29]

$$\Xi[\omega(t)] + \Phi[\omega(t)] = w(t)\,, \qquad n-1 < \sigma \leq n, \tag{70}$$

with boundary condition

$$\mathcal{B}\left[\omega, \frac{\partial \omega}{\partial t}\right] = 0, \tag{71}$$

where the fractional derivative of $\omega(t)$ with Caputo sense is indicated as $\Xi = D_t^{\sigma} = \frac{\partial^{\sigma}}{\partial t^{\sigma}}$ (generic differential operator), the general differential operator is represented by Φ, the nameless function is represented by $\omega(t)$, the known continuous functions are represented by $w(t)$ and the boundary operator is represented by $\mathcal{B}$. Ξ is the main requirement; however, we can combine many linear terms with nonlinear terms as desired.

The initial condition is obtained by removing the nonlinear component

$$D_t^{\alpha}\omega_0(t) = w(t)\,, \qquad \mathcal{B}\left[\omega_0, \frac{\partial\omega_0}{\partial t}\right] = 0. \tag{72}$$

To construct the first iteration of the solution, we'll solve the next equation

$$D_t^{\alpha}\omega_1(t) + \Phi\left[\omega_0(t)\right] = w(t)\,, \qquad \mathcal{B}\left[\omega_1, \frac{\partial\omega_1}{\partial t}\right] = 0. \tag{73}$$

As a result, we have a simple iterative stride $\omega_{n+1}(t)$ that adequately solves a linear and nonlinear series of problems

$$D_t^{\alpha}\omega_{n+1}(t) + \Phi\left[\omega_n(t)\right] = w(t)\,, \qquad \mathcal{B}\left[\omega_{n+1}, \frac{\partial\omega_{n+1}}{\partial t}\right] = 0. \tag{74}$$

It is critical to remember that any of $\omega_{n+1}(t)$ is a discrete solution to the problem when using this method (70).

We confirm that these iterative procedures are simple to perform and that every solution is an improvement on the previous iteration. To ensure that solutions are converging, successive iterations must be checked against the previous iteration.

The analytic solution converges with the exact solution to the issue (70) when more iterations are performed. On this basis, a sufficient agreement between the exact solution and a plausible analytical solution can be found as follows:

$$\omega(t) = \lim_{n\Longrightarrow\infty} \omega_n(t). \tag{75}$$

4.2 2019-nCOV with the Caputo Fractional Derivative

From the SEAIRV model and the initial conditions (2), (4) with the fractional Caputo derivative, we'll use the semi-analytic iterative approach to solve the problem by first rewriting the equation as

$$\begin{cases} \Xi_1(S) = {}^{C}D_t^{\sigma}V = \dfrac{\partial^{\sigma}S}{\partial t^{\sigma}}, & \Phi_1(S) = -\omega S - \beta\left[IS + \eta AS\right] - \beta_1 VS + \rho R, \quad w_1(t) = \Lambda, \\ \Xi_2(E) = {}^{C}D_t^{\sigma}E = \dfrac{\partial^{\sigma}E}{\partial t^{\sigma}}, & \Phi_2(E) = \beta\left[IS + \eta AS\right] + \beta_1 VS - E\left\{k_2(1-\gamma) + k_1\gamma + \omega\right\}, \quad w_2(t) = 0, \\ \vdots & \\ \Xi_6(V) = {}^{C}D_t^{\sigma}V = \dfrac{\partial^{\sigma}V}{\partial t^{\sigma}}, & \Phi_6(V) = m_1 A + m_2 I - \tau V, \quad w_6(t) = 0. \end{cases} \tag{76}$$

The initial issues which should be tackled are

$$\begin{cases} \Xi_1(S_0) = 0, & S(0) = 30416000, \\ \Xi_2(E_0) = 0, & E(0) = 5, \\ \vdots & \\ \Xi_6(V_0) = 0, & V(0) = 0. \end{cases} \tag{77}$$

Eq. (77) can be solved using a simple treatment, as seen below:

$$\begin{cases} I^{\sigma}\left({}^{C}D_{t}^{\sigma}S_{0}\right)=0, & S(0)=30416000,\\ I^{\sigma}\left({}^{C}D_{t}^{\sigma}E_{0}\right)=0, & E(0)=5,\\ \vdots & \\ I^{\sigma}\left({}^{C}D_{t}^{\sigma}V_{0}\right)=0, & V(0)=0. \end{cases} \tag{78}$$

As a result of the fundamental properties of Definition 1, the initial iteration is

$$\begin{cases} S_{0}(t)=30416000+\dfrac{\Lambda t^{\sigma}}{\Gamma(\sigma+1)},\\ E_{0}(t)=5,\\ A_{0}(t)=5,\\ I_{0}(t)=2,\\ R_{0}(t)=0,\\ V_{0}(t)=0. \end{cases} \tag{79}$$

We can now calculate the next iteration

$$\begin{cases} \Xi_{1}\left(S_{1}\right)+\Phi\left(S_{0}(t)\right)+w(t)=0, & S_{1}(0)=30416000+\dfrac{\Lambda t^{\sigma}}{\Gamma(\sigma+1)},\\ \Xi_{2}\left(E_{1}\right)+\Phi\left(E_{0}(t)\right)+w(t)=0, & E_{1}(0)=5,\\ \vdots & \\ \Xi_{6}\left(V_{1}\right)+\Phi\left(V_{0}(t)\right)+w(t)=0, & V_{1}(0)=0. \end{cases} \tag{80}$$

Then, by integrating both sides of Eq. (80) and using the fundamental properties of Definition 2, we arrive at

$$\begin{cases} I^{\sigma}\left({}^{C}D_{t}^{\sigma}S_{1}(t)\right)=I^{\sigma}\left(\Lambda-\omega S_{0}-\beta\left[I_{0}S_{0}+\eta A_{0}S_{0}\right]-\beta_{1}V_{0}S_{0}+\rho R_{0}\right), & S_{1}(0)=30416000+\dfrac{\Lambda t^{\sigma}}{\Gamma(\sigma+1)},\\ I^{\sigma}\left({}^{C}D_{t}^{\sigma}E_{1}(t)\right)=I^{\sigma}\left(\beta\left[I_{0}S_{0}+\eta A_{0}S_{0}\right]+\beta_{1}V_{0}S_{0}-E_{0}\left\{k_{2}(1-\gamma)+k_{1}\gamma+\omega\right\}\right), & E_{1}(0)=5,\\ \vdots \quad \vdots & \\ I^{\sigma}\left({}^{C}D_{t}^{\sigma}V_{1}(t)\right)=I^{\sigma}\left(m_{1}A_{0}+m_{2}I_{0}-\tau V_{0}\right), & V_{1}(0)=0. \end{cases} \tag{81}$$

Then, we get the subsequent iteration as

$$S_{1}(t)=30416000+\frac{1334.06t^{\sigma}}{\Gamma(\sigma+1)}-\frac{0.0565841t^{2\sigma}}{\Gamma(2\sigma+1)},\quad E_{1}(t)=5+\frac{8.68617t^{\sigma}}{\Gamma(\sigma+1)}+\frac{0.00041116t^{2\sigma}}{\Gamma(2\sigma+1)}, \tag{82}$$

$$A_{1}(t)=5-\frac{3.21697t^{\sigma}}{\Gamma(\sigma+1)},\quad I_{1}(t)=2-\frac{0.163526t^{\sigma}}{\Gamma(\sigma+1)},\quad R_{1}(t)=\frac{4.1586t^{\sigma}}{\Gamma(\sigma+1)},\quad V_{1}(t)=\frac{1.932t^{\sigma}}{\Gamma(\sigma+1)}. \tag{83}$$

The following iteration is calculable and is provided as

$$\begin{cases} \Xi_1(S_2) + \Phi(S_1(t)) + w(t) = 0, & S_2(0) = 30416000 + \dfrac{\Lambda t^{\sigma}}{\Gamma(\sigma+1)}, \\ \Xi_2(E_2) + \Phi(E_1(t)) + w(t) = 0, & E_2(0) = 5, \\ \vdots & \\ \Xi_6(V_2) + \Phi(V_1(t)) + w(t) = 0, & V_2(0) = 0. \end{cases} \tag{84}$$

By integrating both sides of Eq. (84) and using the fundamental properties of Definition 2, we arrive at

$$\begin{cases} I^{\sigma}\left({}^{C}D_t^{\sigma} S_2(t)\right) = I^{\sigma}\left(\Lambda - \omega S_1 - \beta\left[I_1 S_1 + \eta A_1 S_1\right] - \beta_1 V_1 S_1 + \rho R_1\right), & S_2(0) = 30416000 + \dfrac{\Lambda t^{\sigma}}{\Gamma(\sigma+1)}, \\ I^{\sigma}\left({}^{C}D_t^{\sigma} E_2(t)\right) = I^{\sigma}\left(\beta\left[I_1 S_1 + \eta A_1 S_1\right] + \beta_1 V_1 S_1 - E_1\left\{k_2(1-\gamma) + k_1\gamma + \omega\right\}\right), & E_2(0) = 5, \\ \vdots \qquad\qquad \vdots & \\ I^{\sigma}\left({}^{C}D_t^{\sigma} V_2(t)\right) = I^{\sigma}\left(m_1 A_1 + m_2 I_1 - \tau V_1\right), & V_2(0) = 0. \end{cases} \tag{85}$$

Then, we get the subsequent iteration as

$$\begin{aligned} S_2(t) = {} & 30416000 + \frac{2.426 \times 10^{-6} t^{3\sigma}}{\Gamma(3\sigma+1)} + \frac{7.38716 \times 10^{-5}\Gamma(2\sigma+1) t^{3\sigma}}{\Gamma(\sigma+1)^2\Gamma(3\sigma+1)} + \frac{14.7624 t^{\sigma}}{\Gamma(\sigma+1)} \\ & + \frac{t^{\sigma}}{\Gamma(\sigma+1)}\left(1319.29 - \frac{3.1332 \times 10^{-9}\Gamma(3\sigma+1) t^{3\sigma}}{\Gamma(2\sigma+1)\Gamma(4\sigma+1)} + \frac{5.916114^{-\sigma} t^{\sigma}}{\Gamma\left(\sigma+\frac{1}{2}\right)}\right), \end{aligned} \tag{86}$$

$$\begin{aligned} E_2(t) = {} & 5 + \frac{8.68617 t^{\sigma}}{\Gamma(\sigma+1)} + t^{2\sigma} \times \\ & \left(\frac{t^{\sigma}\left(-\dfrac{7.38716 \times 10^{-5}\Gamma(2\sigma+1)}{\Gamma(\sigma+1)^2} + \dfrac{3.1332 \times 10^{-9}\Gamma(3\sigma+1)^2 t^{\sigma}}{\Gamma(\sigma+1)\Gamma(2\sigma+1)\Gamma(4\sigma+1)} - 6.52288 \times 10^{-5}\right)}{\Gamma(3\sigma+1)}\right. \\ & \left. - \frac{5.426334^{-\sigma}}{\Gamma\left(\sigma+\frac{1}{2}\right)\Gamma(\sigma+1)}\right), \end{aligned} \tag{87}$$

$$A_2(t) = 5 - \frac{3.21697t^{\sigma}}{\Gamma(\sigma+1)} + \frac{6.909864^{-\sigma}t^{2\sigma}}{\Gamma\left(\sigma+\frac{1}{2}\right)\Gamma(\sigma+1)} + \frac{6.31669\times 10^{-5}t^{3\sigma}}{\Gamma(3\sigma+1)},$$
$$R_2(t) = t^{\sigma}\left(\frac{4.1586}{\sigma\Gamma(\sigma)} - \frac{7.597224^{-\sigma}t^{\sigma}}{\Gamma\left(\sigma+\frac{1}{2}\right)\Gamma(\sigma+1)}\right), \tag{88}$$
$$I_2(t) = 2 - \frac{0.163526t^{\sigma}}{\Gamma(\sigma+1)} + \frac{0.0982714^{-\sigma}t^{2\sigma}}{\Gamma\left(\sigma+\frac{1}{2}\right)\Gamma(\sigma+1)} + \frac{2.026\times 10^{-6}t^{3\sigma}}{\Gamma(3\sigma+1)},$$
$$V_2(t) = t^{\sigma}\left(\frac{1.932}{\Gamma(\sigma+1)} - \frac{1.435964^{-\sigma}t^{\sigma}}{\Gamma\left(\sigma+\frac{1}{2}\right)\Gamma(\sigma+1)}\right). \tag{89}$$

Each iteration of $\omega_n(t)$ appears an analytical solution to the model (4), according to Eq. (75). The analytical solution gets closer to the exact solution as the number of iterations increases. For the analytical solution, we satisfy the following series template as

$$\omega(t) = \lim_{n\Longrightarrow\infty}\omega_n(t) \simeq \omega_2(t), \tag{90}$$

where $\omega_2(t)$ represents both $S_2(t)$ or $E_2(t)$ or $A_2(t)$ or $I_2(t)$ or $R_2(t)$ or $V_2(t)$.

Using the approach described in (13), we shall provide an example of the fractional analytical solution's convergence analysis.

We get the following results:

$$\mu_0(S) = 30416000 + \frac{1319.29t^{\sigma}}{\Gamma(\sigma+1)},\ \mu_1(S) = t^{\sigma}\left(\frac{14.7624}{\Gamma(\sigma+1)} - \frac{0.0565841t^{\sigma}}{\Gamma(2\sigma+1)}\right),\ \mu_2(S) = S_2(t) - S_1(t), \cdots, \tag{91}$$

$$\mu_0(E) = 5,\ \mu_1(E) = \frac{0.00041116t^{2\sigma}}{\Gamma(2\sigma+1)} + \frac{8.68617t^{\sigma}}{\Gamma(\sigma+1)},\ \mu_2(E) = E_2(t) - E_1(t), \cdots, \tag{92}$$

$$\vdots$$

$$\mu_0(V) = 0, \mu_1(V) = \frac{1.932t^{\sigma}}{\Gamma(\sigma+1)},\ \mu_2(V) = -\frac{1.435964^{-\sigma}t^{2\sigma}}{\Gamma\left(\sigma+\frac{1}{2}\right)\Gamma(\sigma+1)}, \cdots. \tag{93}$$

We obtain the next C_n's by using the above iterations and calculating amount of C_n for the present problem

$$C_n = \frac{\|\mu_{n+1}(t)\|}{\|\mu_n(t)\|}, n = 0, 1, 2, \cdots, \tag{94}$$

where $n \geq 0$, $\forall(t) : t \in \mathbb{I}$ and the C_n's are less than one as shown in Table 2.

Table 2: Compute the convergence analysis of FTAM solutions for SEAIRV model with Caputo and ABC fractional derivatives

		Caputo fractional derivative		ABC fractional derivative	
		C_0	C_1	C_0	C_1
$\sigma = 1.00$	S	2.42436514E–7	0.0575394830	2.4243651E–7	0.0575394830
	E	0.5211741272	0.0528752651	0.5211741272	0.0528752651
	A	0.1930182354	0.1817771251	0.1930182354	0.1817771251
	I	0.0408815140	0.0847629770	0.0408815140	0.0847629770
	R	∞	0.2576751384	∞	0.2576751384
	V	∞	0.1048338169	∞	0.1048338169
$\sigma = 0.90$	S	2.466621152E–6	0.2530232067	2.7010642E–7	0.0707723101
	E	0.7238224105	0.0851692880	0.6112266552	0.0684287355
	A	0.2680714738	0.3741911346	0.2263689578	0.2352477763
	I	0.04917812291	0.1403858674	0.0455575779	0.1042336974
	R	∞	0.4267684956	∞	0.3168645733
	V	∞	0.1736285875	∞	0.1289147368
$\sigma = 0.80$	S	4.615470918E–6	0.3054983529	2.9885890E–7	0.0861621950
	E	0.9169772509	0.0724100400	0.7119212540	0.0876525941
	A	0.3396073948	0.5426301120	0.2636607139	0.3013368372
	I	0.05668874144	0.1882753102	0.0504201698	0.1268675606
	R	∞	0.5723508527	∞	0.3856693971
	V	∞	0.2328580276	∞	0.1569076288

4.3 2019-nCOV with the ABC Fractional Derivative

From the SEAIRV model and the initial conditions (2), (5) with the ABC derivative, we'll use the semi-analytic iterative approach to solve the problem by first rewriting the equation as

$$\begin{cases} \Xi_1(S) = {}^{ABC}D_t^{\sigma} V = \dfrac{\partial^{\sigma} S}{\partial t^{\sigma}}, \\ \quad \Phi_1(S) = -\omega S - \beta\left[IS + \eta AS\right] - \beta_1 VS + \rho R, \\ \quad w_1(t) = \Lambda, \\ \Xi_2(E) = {}^{ABC}D_t^{\sigma} E = \dfrac{\partial^{\sigma} E}{\partial t^{\sigma}}, \\ \quad \Phi_2(E) = \beta\left[IS + \eta AS\right] + \beta_1 VS - E\left\{k_2(1-\gamma) + k_1\gamma + \omega\right\}, \\ \quad w_2(t) = 0, \\ \quad \vdots \\ \Xi_6(V) = {}^{ABC}D_t^{\sigma} V = \dfrac{\partial^{\sigma} V}{\partial t^{\sigma}}, \\ \quad \Phi_6(V) = m_1 A + m_2 I - \tau V, \\ \quad w_6(t) = 0. \end{cases} \tag{95}$$

The initial issues should be tackled are

$$\begin{cases} \Xi_1(S_0) = 0, \quad S_0(0) = 30416000 + \Lambda\left((1-\sigma) + \dfrac{\sigma t^{\sigma}}{\Gamma(\sigma+1)}\right), \\ \Xi_2(E_0) = 0, \quad E_0(0) = 5, \\ \vdots \\ \Xi_6(V_0) = 0, \quad V_0(0) = 0. \end{cases} \tag{96}$$

Stratifying the same basal concept of the TAM of fractional order, we get the next analytical solutions

$$S_1(t) = 3.04173 \times 10^7 + (-0.0565841\sigma - 1333.94)\sigma + \sigma t^{\sigma}\left(\frac{2653.29 - 1319.24\sigma}{\Gamma(\sigma+1)} - \frac{0.0565841\sigma t^{\sigma}}{\Gamma(2\sigma+1)}\right), \tag{97}$$

$$E_1(t) = 13.6866 + (0.00041116\sigma - 8.687)\sigma + \sigma t^{\sigma}\left(\frac{1327.98 - 1319.29\sigma}{\Gamma(\sigma+1)} + \frac{0.00041116\sigma t^{\sigma}}{\Gamma(2\sigma+1)}\right), \tag{98}$$

$$A_1(t) = 5 - 3.21697\left(1 - \sigma + \frac{\sigma t^{\sigma}}{\Gamma(\sigma+1)}\right), \qquad I_1(t) = 2 - 0.163526\left(1 - \sigma + \frac{\sigma t^{\sigma}}{\Gamma(\sigma+1)}\right), \tag{99}$$

$$R_1(t) = 4.1586\left(1 - \sigma + \frac{\sigma t^{\sigma}}{\Gamma(\sigma+1)}\right), \qquad V_1(t) = 1.932\left(1 - \sigma + \frac{\sigma t^{\sigma}}{\Gamma(\sigma+1)}\right), \cdots \tag{100}$$

Each iteration of $\omega_n(t)$ appears an analytical solution to the model (5), according to Eq. (75). The analytical solution gets closer to the exact solution as the number of iterations increases. We complete the following analytic solution series template as

$$\omega(t) = \lim_{n \Longrightarrow \infty} \omega_n(t) \simeq \omega_2(t). \tag{101}$$

We will demonstrate the convergence analysis for the fractional approximate solution using the method given in (13). We get the following results:

$$\begin{aligned} &\mu_0(S) = S_0 = 30416000 + \Lambda\left((1-\sigma) + \frac{\sigma t^{\sigma}}{\Gamma(\sigma+1)}\right), \\ &\mu_1(S) = 14.7058 - (0.0565841\sigma^2 + 14.6492\sigma)\frac{\sigma(1334 - 1319.24\sigma)t^{\sigma}}{\Gamma(\sigma+1)} - \frac{0.0565841\sigma^2 t^{2\sigma}}{\Gamma(2\sigma+1)}, \cdots \end{aligned} \tag{102}$$

$$\begin{aligned} \mu_0(E) = E_0 = 5, \quad \mu_1(E) =& 8.68658 + (0.00041116\sigma - 8.687\sigma)\sigma \\ &+ t^{\sigma}\left(\frac{1327.98 - 1319.29\sigma}{\Gamma(\sigma+1)} + \frac{0.00041116\sigma t^{\sigma}}{\Gamma(2\sigma+1)}\right), \cdots \end{aligned} \tag{103}$$

$$\vdots$$

$$\mu_0(V) = V_0 = 0, \quad \mu_1(V) = 1.932\left(1 - \sigma + \frac{\sigma t^{\sigma}}{\Gamma(\sigma+1)}\right), \cdots \tag{104}$$

Using the aforementioned iterations we determine the subsequent C_n's and determining the quantity of C_n for the current issue

$$C_n = \frac{\|\lambda_{n+1}(t)\|}{\|\lambda_n(t)\|}, \qquad n = 0, 1, 2, \cdots \tag{105}$$

where $n \geq 0$, $\forall(t) : t \in \mathbb{I}$, and the C_n's are less than one as shown in Table 2.

5 Analysis and Discussion

In this study, we utilized two distinct fractional operators, the Caputo and Atangana-Baleanu in Caputo sense (ABC) derivatives, to model the COVID-19 epidemic. While both fractional operators allow for the inclusion of memory effects in the system dynamics, our results indicate that the ABC derivative provides more detailed insights than the Caputo derivative. The ABC derivative is characterized by a non-singular kernel, which enables it to capture both short-term and long-term memory effects more effectively than the Caputo derivative, which primarily focuses on short-term memory.

This property of the ABC derivative becomes particularly important in the context of epidemiological models, where past states, such as infection and recovery rates, have lingering effects on the future course of the epidemic. The long-term memory characteristics embedded in the ABC derivative allow it to simulate the gradual and complex evolution of the epidemic, offering a more comprehensive understanding of the disease's progression over time.

Our simulations demonstrate that the ABC fractional model fits the clinical data more accurately than the Caputo model. Specifically, the ABC model shows smoother transitions and more gradual changes that align closely with observed real-world data. This is critical in epidemic modeling, as abrupt changes in state variables, such as infection and recovery rates, are not typically observed in real-life scenarios. The ability of the ABC model to reflect this gradual change is one of its key strengths.

In our comparative analysis, we simulated the epidemic model using both the Caputo and ABC fractional derivatives under various parameter settings. The results reveal that the ABC model consistently maintains accuracy and stability over a wider range of conditions, particularly when modeling the long-term behavior of the epidemic. For instance, when simulating infection rates and recovery dynamics over extended periods, the Caputo model exhibited sharper transitions and was less adaptable to changes in the system, especially when parameter values varied significantly. In contrast, the ABC model demonstrated a more robust response, accurately reflecting the memory effects and adapting to the parameter variations without significant deviations from the expected behavior.

Figs. 1 and 2 illustrate this comparison. The graphs show that, under identical initial conditions, the ABC model converges more smoothly to equilibrium and better captures the gradual decline in infection rates. These results substantiate our claim that the ABC derivative offers a more accurate and comprehensive representation of memory effects in the system compared to the Caputo derivative.

From Table 2, all FTAM solutions converge because all the values of $C_n's$ at different values of a are less than one. We note that the past has a greater impact on the model reflecting the Mittag-Leffler type kernel and as compared to the classical and Caputo fractional derivatives, has the highest convergence. Figs. 3–8 show the new fractional coronavirus (2019-nCOV) geometric component solutions at different values sv using two fractional derivatives (Caputo-ABC). Actually, we can easily see that the derived analytical solutions are continually dependent on the fractional derivative σ. Figs. 1 and 2 show the new fractional coronavirus (2019-nCOV) geometric component solutions at

$\sigma = 0.80$. Evidence suggests that ABC fractional derivatives reveal more information for comparison with clinical data.

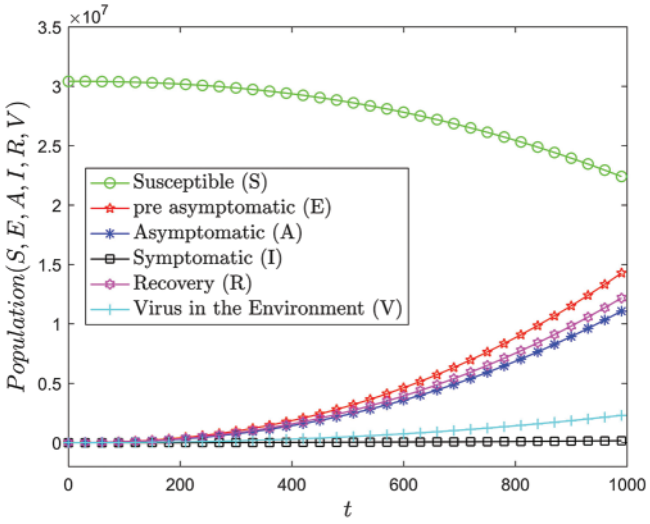

Figure 1: Variance of populace concentration *vs.* time for Caputo fractional derivative at $\sigma = 0.80$

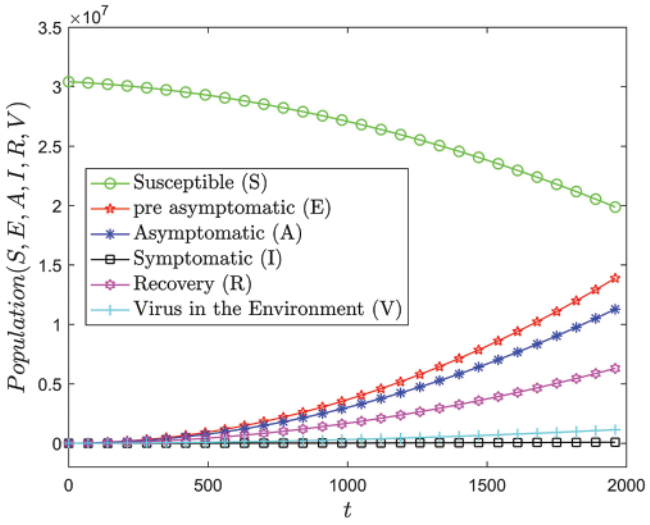

Figure 2: Variance of populace concentration *vs.* time for A–B fractional derivative in Caputo sense at $\sigma = 0.80$

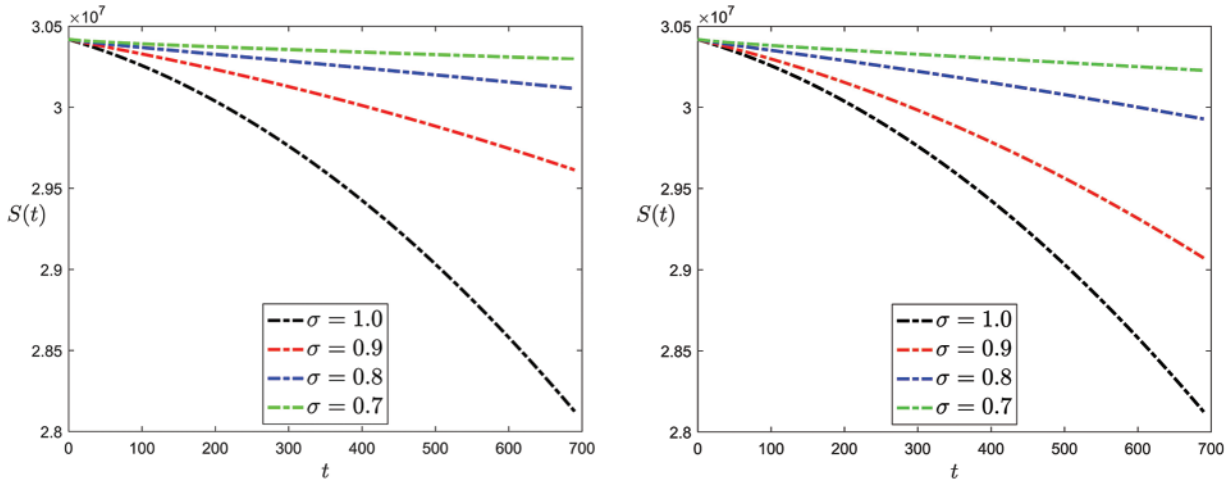

(a) Caputo fractional derivative. (b) ABC fractional derivative.

Figure 3: Comparison of behaviour solution between Caputo and ABC fractional derivatives for susceptible population $S(t)$

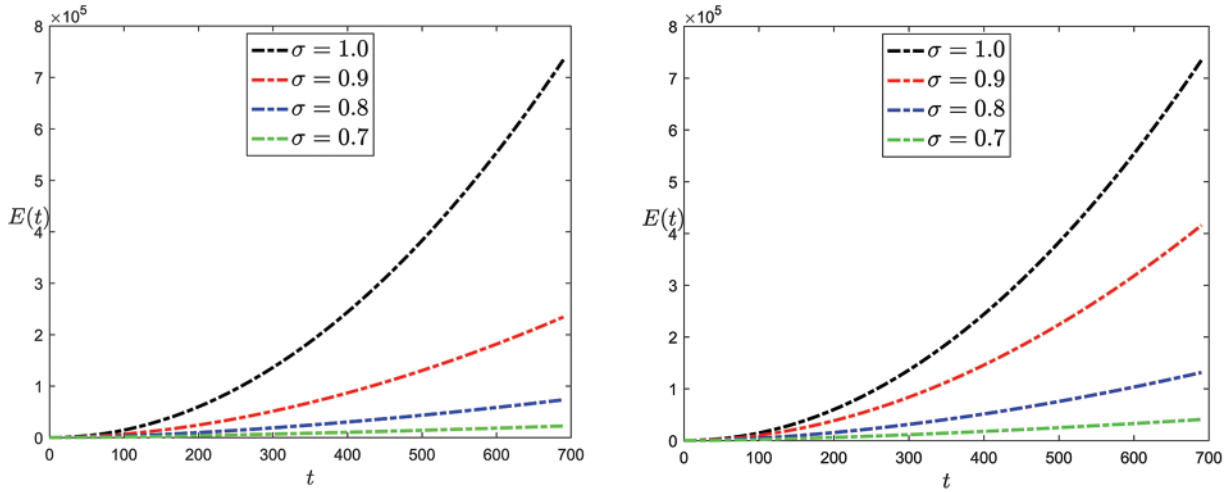

(a) Caputo fractional derivative. (b) ABC fractional derivative.

Figure 4: Comparison of behaviour solution between Caputo and ABC fractional derivatives for Pre-asymptomatic $E(t)$

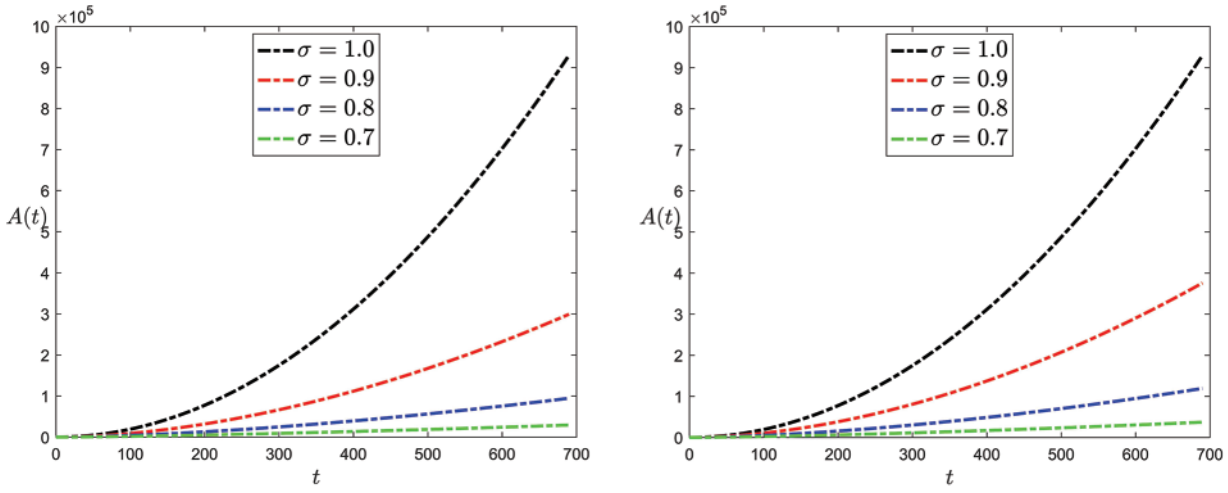

(a) Caputo fractional derivative. (b) ABC fractional derivative.

Figure 5: Comparison of behaviour solution between Caputo and ABC fractional derivatives for asymptomatic population $A(t)$

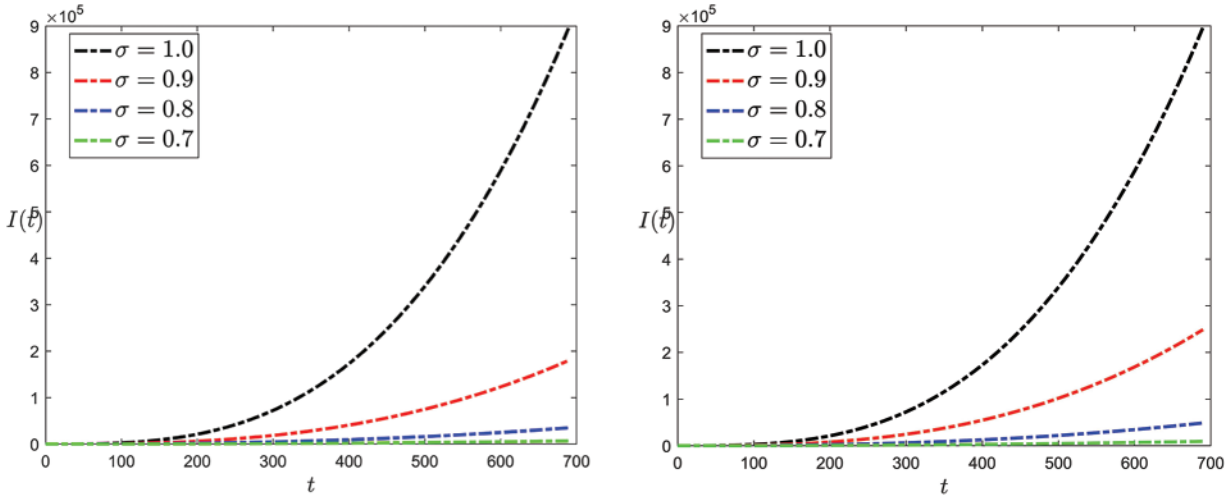

(a) Caputo fractional derivative. (b) ABC fractional derivative.

Figure 6: Comparison of behaviour solution between Caputo and ABC fractional derivatives for symptomatic population $I(t)$

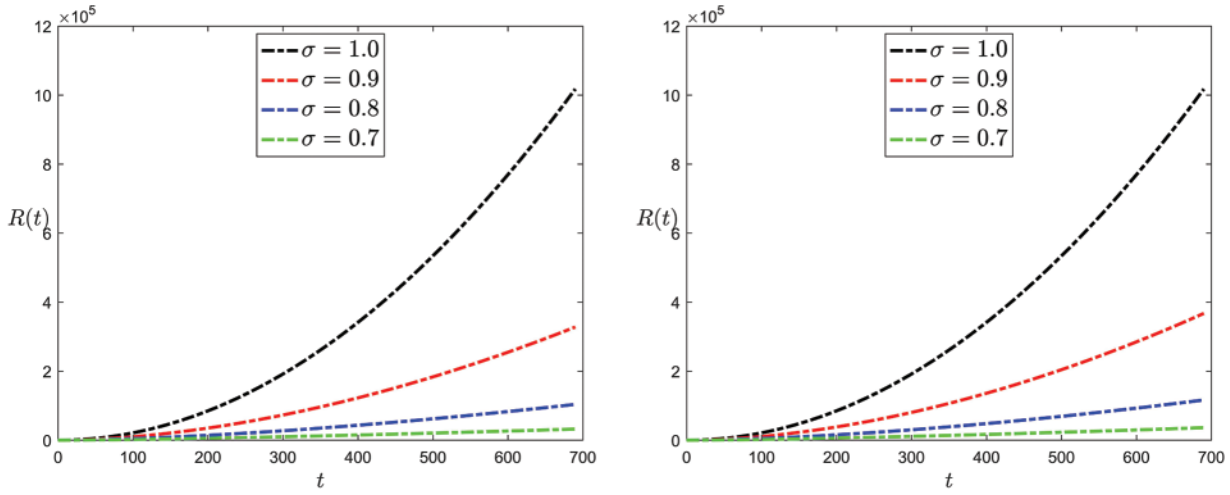

(a) Caputo fractional derivative. (b) ABC fractional derivative.

Figure 7: Comparison of behaviour solution between Caputo and ABC fractional derivatives for recovery population $R(t)$

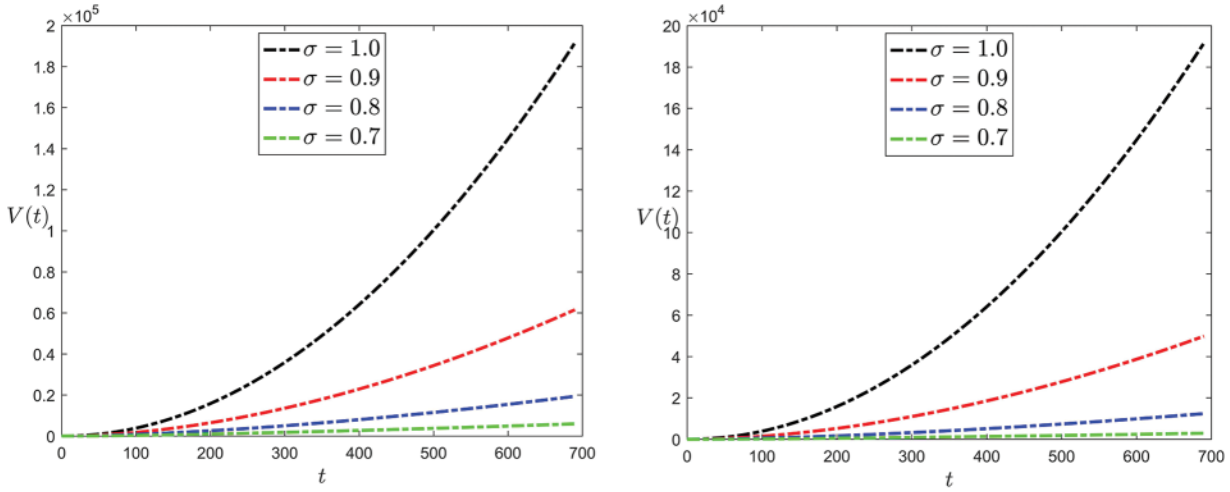

(a) Caputo fractional derivative. (b) ABC fractional derivative.

Figure 8: Comparison of behaviour solution between Caputo and ABC fractional derivatives for virus on surfaces in the environment $V(t)$

6 Conclusion

In this paper, we have studied a new fractional coronavirus (2019-nCOV) model using two fractional derivatives namely the Caputo fractional derivative and the ABC fractional derivative. The convergence analysis, existence and uniqueness of solutions with ABC fractional derivative have been established. In addition, we study the sensibility analysis of reproduction number ($\mathcal{R}_0$) without control. The numerical results of the proposed fractional model were obtained using the FTAM. We have observed that the COVID-19 model can effectively be modeled with fractional derivatives operators.

It is noted that memory features in the ABC derivative are of a more general nature than in the Caputo derivative. It's an excellent mathematical tool explaining how complex systems store memory and inherit certain traits. Comparatively, fractional models' basic solutions continue to show practical scaling characteristics that draw users in.

Acknowledgement: Not applicable.

Funding Statement: Princess Nourah bint Abdulrahman University Researchers Supporting Project number (PNURSP2025R518), Princess Nourah bint Abdulrahman University, Riyadh, Saudi Arabia.

Author Contributions: The authors confirm contribution to the paper as follows: study conception and design: Anas Arafa; data collection: Zuhur Alqahtani; analysis and interpretation of results: Ahmed Hagag; draft manuscript preparation: Ahmed Hagag, Zuhur Alqahtani, and Anas Arafa. All authors reviewed the results and approved the final version of the manuscript.

Availability of Data and Materials: No data were used to support this study.

Ethics Approval: Not applicable.

Conflicts of Interest: The authors declare no conflicts of interest to report regarding the present study.

References

1. Waziri AS, Massawe ES, Makinde OD. Mathematical modelling of hiv/aids dynamics with treatment and vertical transmission. Appl Math. 2012;2(3):77–89.
2. Diekmann O, Heesterbeek J, Roberts MG. The construction of next-generation matrices for compartmental epidemic models. J R Soc Interf. 2010;7(47):873–85.
3. Kumar S, Chauhan R, Momani S, Hadid S. Numerical investigations on COVID-19 model through singular and non-singular fractional operators. Numer Methods Partial Differ Equ. 2024;40(1):e22707.
4. Kumar S, Kumar R, Momani S, Hadid S. A study on fractional COVID-19 disease model by using hermite wavelets. Math Methods Appl Sci. 2023;46(7):7671–87.
5. Keeling MJ, Rohani P. Modeling infectious diseases in humans and animals. Princeton, NJ, USA: Princeton University Press; 2008.
6. Lu H, Stratton CW, Tang YW. Outbreak of pneumonia of unknown etiology in Wuhan, China: The mystery and the miracle. J Med Virol. 2020;92(4):401–2. doi:10.1002/jmv.25678.
7. Ji W, Wang W, Zhao X, Zai J, Li X. Homologous recombination within the spike glycoprotein of the newly identified coronavirus may boost cross-species transmission from snake to human. J Med Virol. 2020;92(4):433–40. doi:10.1002/jmv.25682.
8. Organization WH. Novel coronavirus (2019-nCOV) situation report-26. Geneva, Switzerland: World Health Organization; 2020. vol. 13, no. 2.
9. Service GH. COVID-19: Ghanaâs outbreak response management updates. 2020. Available from: https://ghanahealthservice.org/covid19/archive.php. [Accessed 2024].
10. Asamoah JKK, Owusu MA, Jin Z, Oduro F, Abidemi A, Gyasi EO. Global stability and cost-effectiveness analysis of COVID-19 considering the impact of the environment: using data from Ghana. Chaos, Solit Fract. 2020;140:110103.
11. Review WP. Total population. 2020. Available from: https://worldpopulationreview.com/. [Accessed 2020].
12. World Bank. Life expectancy at birth, total (years)-Ghana. 2020. Available from: https://data.worldbank.org/indicator/SP.DYN.LE00.IN?locations=GH. [Accessed 2020].

13. Coronavirus Resource Center. How long can the coronavirus that causes COVID-19 survive on surfaces?. 2020. Available from: https://www.health.harvard.edu/diseases-and-conditions/covid-19-basics. [Accessed 2020].
14. Zhao S, Chen H. Modeling the epidemic dynamics and control of COVID-19 outbreak in China. Quant Biol. 2020;8(1):11–9.
15. Rajagopal K, Hasanzadeh N, Parastesh F, Hamarash II, Jafari S, Hussain I. A fractional-order model for the novel coronavirus (COVID-19) outbreak. Nonlinear Dyn. 2020;101:711–8.
16. Jin B. Fractional differential equations. Cham, Switzerland: Springer International Publishing; 2021.
17. Baleanu D, Diethelm K, Scalas E, Trujillo JJ. Fractional calculus: models and numerical methods. World Scientific. 2012;3:1–476.
18. Arafa A, Hagag A. A new semi-analytic solution of fractional sixth order ~~drinfeld–sokolov–satsuma–hirota~~ equation. Numer Methods Partial Differ Equ. 2022;38(3):372–89.
19. Ahmed N, Macías-Díaz JE, Raza A, Baleanu D, Rafiq M, Iqbal Z, et al. Design, analysis and comparison of a nonstandard computational method for the solution of a general stochastic fractional epidemic model. Axioms. 2021;11(1):10. doi:10.3390/axioms11010010.
20. Arafa AA, Hagag AMS. A new analytic solution of fractional coupled ramani equation. Chin J Phys. 2019;60(6):388–406. doi:10.1016/j.cjph.2019.05.011.
21. Odibat Z, Kumar S. A robust computational algorithm of homotopy asymptotic method for solving systems of fractional differential equations. J Comput Nonlinear Dyn. 2019;14(8):081004. doi:10.1115/1.4043617.
22. Iqbal Z, Macías-Díaz JE, Ahmed N, Javaid A, Rafiq M, Raza A. Analytical and numerical boundedness of a model with memory effects for the spreading of infectious diseases. Symmetry. 2022;14(12):2540. doi:10.3390/sym14122540.
23. Kudu M. A parameter uniform difference scheme for the parameterized singularly perturbed problem with integral boundary condition. Adv Differ Equ. 2018;2018(1):1–12. doi:10.1186/s13662-018-1620-0.
24. Sattar AM, Ertuğrul ÖF, Gharabaghi B, McBean EA, Cao J. Extreme learning machine model for water network management. Neural Comput Appl. 2019;31(1):157–69. doi:10.1007/s00521-017-2987-7.
25. Arafa A, Hagag A. Approximate solutions for some reaction–diffusion systems with non integer order. Int J Appl Comput Math. 2021;7(1):1–22. doi:10.1007/s40819-021-00957-z.
26. Odibat Z, Momani S. A generalized differential transform method for linear partial differential equations of fractional order. Appl Math Lett. 2008;21(2):194–9. doi:10.1016/j.aml.2007.02.022.
27. Arafa AA, Hagag AMS. Q-homotopy analysis transform method applied to fractional ~~kundu–eckhaus~~ equation and fractional massive thirring model arising in quantum field theory. Asian-Eur J Math. 2019;12(3):1950045. doi:10.1142/S1793557119500451.
28. Temimi H, Ansari AR. A new iterative technique for solving nonlinear second order multi-point boundary value problems. Appl Math Comput. 2011;218(4):1457–66. doi:10.1016/j.amc.2011.06.029.
29. Arafa AA, El-Sayed AM, Hagag AMSH. A fractional temimi-ansari method (FTAM) with convergence analysis for solving physical equations. Math Methods Appl Sci. 2021;44(8):6612–29. doi:10.1002/mma.7212.
30. Temimi H, Ansari AR. A semi-analytical iterative technique for solving nonlinear problems. Comput Mathemat Appl. 2011;61(2):203–10. doi:10.1016/j.camwa.2010.10.042.
31. Atangana A, Baleanu D. New fractional derivatives with nonlocal and non-singular kernel: theory and application to heat transfer model. arXiv preprint arXiv:1602.03408. 2016.
32. Akgül A. A novel method for a fractional derivative with non-local and non-singular kernel. Chaos, Solit Fract. 2018;114(2):478–82. doi:10.1016/j.chaos.2018.07.032.
33. Odibat ZM. A study on the convergence of variational iteration method. Math Comput Model. 2010;51(9–10):1181–92. doi:10.1016/j.mcm.2009.12.034.